E 5

NACA RM L51H01

NACA

RESEARCH MEMORANDUM

ANALYSIS OF LONGITUDINAL STABILITY AND TRIM OF THE BELL X-1 AIRPLANE AT A LIFT COEFFICIENT OF 0.3 TO MACH NUMBERS NEAR 1.05

By Hubert M. Drake, John R. Carden, and
Harry P. Clagett

Langley Aeronautical Laboratory
Langley Field, Va.

NATIONAL ADVISORY COMMITTEE
FOR AERONAUTICS

WASHINGTON

October 9, 1951
Declassified August 16, 1957

NATIONAL ADVISORY COMMITTEE FOR AERONAUTICS

RESEARCH MEMORANDUM

ANALYSIS OF LONGITUDINAL STABILITY AND TRIM OF THE BELL X-1 AIRPLANE AT A LIFT COEFFICIENT OF 0.3 TO MACH NUMBERS NEAR 1.05

By Hubert M. Drake, John R. Carden, and
Harry P. Clagett

SUMMARY

Flight test data have been obtained with the two Bell X-1 airplanes, the X-1-1 airplane having an 8-percent-thick wing and a 6-percent-thick tail and the X-1-2 airplane having a 10-percent-thick wing and an 8-percent-thick tail. Sufficient data have been obtained on these airplanes to permit an analysis of the variation of longitudinal stability to a Mach number of about 1.05 and of longitudinal trim to a Mach number of 1.0. The data were obtained from those portions of the flights in which the lift coefficient was between 0.25 and 0.35. The test altitudes were between 40,000 feet and 50,000 feet.

It was found that the downwash factor $d\epsilon/d\alpha$ decreased from 0.59 at a Mach number of 0.80 to a minimum value of -0.19 at a Mach number of 0.925 followed by an increase to 0.20 at a Mach number of 1.0. The tail total-pressure ratio varied but little with Mach number. The contribution of the fuselage to the static stability of the airplane was small. The variation of the stability contribution of the horizontal tail is similar to the variation of the downwash factor $d\epsilon/d\alpha$ and is responsible for the major part of the variation in airplane static stability. The variation in the apparent stability $d\delta_e/dC_{L_A}$ with Mach number was primarily caused by the large decrease in the relative elevator-stabilizer effectiveness except between Mach numbers of 0.89 and 0.96 where the change in static stability, produced by the downwash factor, is the more important. The calculated apparent stability $d\delta_e/dC_{L_A}$ increases from 10° at a Mach number of 0.70 to 213° at a Mach number of 1.0 followed by a decrease to 130° at a Mach number of 1.05.

The positive value of pitching moment for zero stabilizer and elevator decreases with increasing Mach number to a Mach number of 0.87 above which it is approximately constant. The calculated trim curve is in good agreement with the experimentally obtained trim curve.

INTRODUCTION

The National Advisory Committee for Aeronautics is at present conducting flight tests in the transonic speed range with the Bell X-1 airplanes. Two airplanes, differing only in wing and tail thickness, are being used: The X-1-1, having an 8-percent-thick wing and a 6-percent-thick tail is being operated in cooperation with the Air Materiel Command, U. S. Air Force, and the X-1-2, having a 10-percent-thick wing and an 8-percent-thick tail is being operated completely by NACA.

The space available for instrumentation was not sufficient for complete pressure distributions to be obtained on the wing at the same time tail loads were being obtained by strain gages. Therefore, the X-1-1 airplane, which was being used in an exploratory program to obtain maximum Mach number and altitude, was instrumented to measure tail loads with strain gages, while the X-1-2 airplane was instrumented to obtain complete span loadings on the wing from pressure-distribution measurements.

Previous papers, references 1 and 2, have shown that large increases in apparent longitudinal stability and changes in longitudinal trim were encountered at Mach numbers in the transonic range. The present paper gives the results of an analysis made, using the measurements obtained from both X-1 airplanes, to determine the causes of these changes in longitudinal stability and trim. The analysis is restricted to altitudes of about 40,000 feet at which altitude the data utilized were obtained. At lower altitudes large aeroelastic effects would be encountered but insufficient data have been obtained to permit evaluation of these effects.

SYMBOLS

C_L	lift coefficient (L/qS)
C_m	pitching-moment coefficient (M/qSc)
$\left(C_{m_o}\right)_w$	pitching moment of wing at zero lift (M_o/qSc)
c	wing mean aerodynamic chord, feet
g	acceleration due to gravity, 32.2 feet per second^2
i_t	tail incidence angle, degrees
L	lift, pounds

l_t	tail length measured from center of gravity to quarter-chord point of tail, feet
M	pitching moment, foot-pounds
q	dynamic pressure, pounds per square foot $(0.7M^2P)$
q_t	dynamic pressure at tail, pounds per square foot
M	Mach number
P	static pressure, pounds per square foot
S	wing area, square feet
x	distance of center of gravity from aerodynamic center of wing; positive if aerodynamic center is ahead of center of gravity, feet
δ_e	elevator control-surface angle, degrees
ϵ	downwash angle, degrees
α	angle of attack of fuselage center line, degrees
C_{L_α}	slope of lift curve per degree $(dC_L/d\alpha)$

Subscripts:

A	airplane
t	tail alone
w	wing alone
f	fuselage
e	elevator
o	zero lift
c.g.	center of gravity

AIRPLANES AND INSTRUMENTATION

Both X-1 airplanes are geometrically identical except for the thicknesses of the wings and horizontal tails. A sketch of the X-1 configuration is given as figure 1 and the dimensional and mass characteristics are tabulated in table I.

The instrumentation of the two airplanes differs slightly, a complete tabulation being as follows:

X-1-1 airplane	X-1-2 airplane
(8-percent wing, 6-percent tail)	(10-percent wing, 8-percent tail)
3-component accelerometer	3-component accelerometer
Airspeed	Airspeed
Altitude	Altitude
Roll turnmeter	Roll turnmeter
Pitch turnmeter	Pitch turnmeter
Elevator position	Yaw turnmeter
Stabilizer position	Stabilizer position
Right-aileron position	2 aileron positions
Rudder position	Elevator position
Angle of attack	Rudder position
Horizontal-tail strain gages	Wheel and pedal forces
	Angle of sideslip
	2 multiple manometers recording span loading on the left wing

The records were synchronized by a common timer. The airspeed systems were calibrated by the radar method as discussed in reference 3. The elevator position was measured with respect to the stabilizer at the elevator operating arm and the stabilizer position was measured with respect to the airplane center line.

Measurements were made to determine the dynamic pressure at the tail of the X-1-2 airplane by using a small total-pressure tube installed ahead of the leading edge of the horizontal tail at the 50-percent-semispan station. The free-stream static pressure measured at the nose boom was subtracted from this total pressure to give the dynamic pressure at the tail. A photograph of the installation is shown in figure 2.

TESTS

Because of the differences in instrumentation and flight objectives of the two airplanes, different measurements of use in analyzing the longitudinal characteristics were made with each X-1 airplane. The data obtained on each airplane are as follows:

X-1-1 airplane:

(a) Tail loads have been measured using strain gages

(b) The airplane longitudinal stability derivative $dC_m/d\alpha$ has been determined from transient responses (reference 4)

(c) The lift-curve slope has been measured in pull-ups as reported in reference 5

X-1-2 airplane:

(a) The pitching moment and static margin dC_m/dC_L of the wing alone have been determined by span loadings from pressure distributions (references 6 and 7)

(b) The relative elevator-stabilizer effectiveness has been measured from trim curves at various stabilizer angles (reference 2)

(c) The effectiveness of the elevator in producing airplane lift has been measured in turns and pull-ups

(d) Preliminary measurements of q_t/q with Mach number in level flight have been made

(e) Preliminary measurements of the variation of lift-curve slope with Mach number have been made

By using the measured flight data it was possible to determine the contributions of the various portions of the airplane to the stick-fixed stability changes and the trim changes using a minimum of wind-tunnel model data. The flight data used were selected from those portions of the flight during which the lift coefficient was between 0.25 and 0.35.

RESULTS AND DISCUSSION

Stick-fixed stability.- The variation of the static-stability derivative dC_m/dC_L with Mach number for various parts of the X-1 airplane is shown in figure 3. These data are for lift coefficients near 0.3 and a center-of-gravity position of 23.5 percent of the mean aerodynamic chord. In this figure the values of dC_m/dC_L for the wing-fuselage combination were computed by use of unpublished tail-loads data obtained on the X-1-1 airplane in flight and the values of dC_m/dC_L for the entire airplane were obtained from the transient-response data reported in reference 4. The variation of dC_m/dC_L of the wing alone with Mach number was not obtained for the X-1-1 airplane but has been measured by means of pressure distributions on the X-1-2 airplane (references 6 and 7) and on an 8-percent-thick wing on the transonic bump as reported in reference 8. These curves are also presented in figure 3. Because there were no data presented in reference 8 at Mach numbers between 0.8 and 0.9 the curve was interpolated on the basis of the X-1-2 data.

The variation of the lift-curve slope of the X-1-1 airplane with Mach number as measured in flight is reported in reference 5 and the variation is reproduced in figure 4. The measured, but as yet unpublished, variation of C_{L_α} for the X-1-2 is also presented in this figure. As pointed out in reference 5, the measured value of C_{L_α} might be low by as much as 8 percent at subsonic Mach numbers because of the location of the angle-of-attack vane. The lift-curve slope of the horizontal tail of the X-1-1 airplane has not been measured in flight. Therefore $C_{L_{\alpha_t}}$ was estimated, based on the airplane C_{L_α} variations and the data on the effects of aspect ratio and thickness presented in references 9 and 10, and the estimate is presented in figure 4. Also shown in this figure is the variation with Mach number of q_t/q obtained in flight tests of the X-1-2 airplane by using the installation shown in figure 2.

By utilizing the data shown in figures 3 and 4 it is possible to determine the stability contribution of the horizontal tail and fuselage and the variation of the downwash factor $d\epsilon/d\alpha$ with Mach number. The variation with Mach number of the tail contribution to stability is obtained by subtracting the wing-fuselage contribution from the complete airplane variation with Mach number shown in figure 3. The resulting variation of the horizontal-tail contribution to static margin is presented in figure 5 and shows that the stability contribution of the horizontal tail increases about three and one-half times as the Mach number is increased from 0.80 to 0.925. At Mach numbers above 0.925 the tail stability contribution decreases to a value at $M = 1.025$ that is twice the low-speed value.

The variation of the fuselage static-stability contribution including the fuselage interference with Mach number was determined by subtracting the wing-alone contribution (from the bump data of fig. 3) from the contribution of the wing-fuselage combination. This variation is presented in figure 5 and indicates that the destabilizing effect of the fuselage increases from the low-speed value of 0.05 to a maximum of about 0.15 at a Mach number of 0.9. At higher Mach numbers the fuselage contribution first decreases and then increases slightly to a value of about 0.08 at a Mach number of 1.025.

The value of $d\epsilon/d\alpha$ was calculated by the use of the equation defining the tail contribution to static stability given as

$$\left(\frac{dC_m}{dC_L}\right)_t = -\left(1 - \frac{d\epsilon}{d\alpha}\right)\frac{C_{L_{\alpha_t}}}{\left(C_{L_\alpha}\right)_A}\frac{q_t}{q}\frac{S_t}{S}\frac{l_t}{c}$$

or

$$\frac{d\epsilon}{d\alpha} = 1 + \frac{\left(\frac{dC_m}{dC_L}\right)_t}{\frac{C_{L_{\alpha_t}}}{\left(C_{L_\alpha}\right)_A}\frac{q_t}{q}\frac{S_t}{S}\frac{l_t}{c}}$$

This equation, as are the others used in this paper, is based on the assumption of linear characteristics. In the transonic range the derivatives $\left(dC_m/dC_L\right)_W$ and $C_{L_{\alpha_A}}$ are known to be nonlinear at lift coefficients above 0.5 but linear at a lift coefficient of 0.3. The degree of nonlinearity of the other derivatives is not known.

The values of the various terms were obtained from figures 4 and 5 and table I. The resulting variation of $d\epsilon/d\alpha$ with Mach number is shown in figure 5. These results show that $d\epsilon/d\alpha$ has a variation with Mach number similar to that of the static-stability contribution of the horizontal tail indicating that the changes in $d\epsilon/d\alpha$ with Mach number have the greatest effect on the tail contribution. There is a rapid decrease of $d\epsilon/d\alpha$ from the low-speed value of about 0.59 at $M = 0.80$ to a minimum value of -0.19 at a Mach number of 0.925, followed by an increase to a value of about 0.20 at $M = 1.0$. This general variation of $d\epsilon/d\alpha$ at Mach numbers below 0.92 is similar to that obtained in the Langley 8-foot high-speed tunnel tests reported in reference 11. The variation obtained from the tunnel tests is presented in figure 5 for comparison with the flight test data. The tunnel tests were made on a model having a 10-percent wing which probably accounts for some of the difference between the flight and tunnel results.

The variation of relative elevator-stabilizer effectiveness with Mach number for the X-1-2 airplane has been reported in reference 2 and the curve is reproduced in figure 6. These data were obtained by making flights at various stabilizer incidence angles and measuring the elevator angles required for trim. The data shown are for up elevator angles only because, as has been pointed out in reference 2, the control effectiveness varies with elevator position at Mach numbers between 0.94 and 1.0. Also shown in this figure is the variation with Mach number of the lift-curve slope of the horizontal tail of the X-1-2 airplane as estimated from the data of figure 4 and references 9 and 10. For convenience, the variation of C_{L_α} with Mach number for the entire X-1-2 airplane obtained in flight tests has been repeated in this figure.

The data available enable a computation of the total stability $\left(dC_m/dC_L\right)_A$ of the X-1-2 airplane. The stability contribution dC_m/dC_L of the wing-fuselage combination is computed by adding the contribution of the fuselage (fig. 5) to the dC_m/dC_L of the wing alone as obtained from the wing-pressure distributions (fig. 3). The resulting variation with Mach number of dC_m/dC_L for the wing plus fuselage is given in figure 7 for a center-of-gravity position of 22 percent mean aerodynamic chord. This variation of dC_m/dC_L for the X-1-2 wing plus fuselage is not appreciably different from that measured for the X-1-1 airplane and shown in figure 3.

In computing the tail contribution to $\left(dC_m/dC_L\right)_A$ the effect of changes in $d\epsilon/d\alpha$ was determined separately by holding the term $\left(1 - \frac{d\epsilon}{d\alpha}\right)$ constant at the value of 0.59 which occurs at $M = 0.80$, and by using the variation shown in figure 5. These two calculated curves are shown in figure 7 and indicate the extent the variation in $d\epsilon/d\alpha$ is responsible for the large changes with Mach number in the dC_m/dC_L contribution of the tail. The variation of q_t/q and $C_{L_{\alpha_t}}/C_{L_{\alpha_A}}$ has very little effect on the tail contribution to dC_m/dC_L.

The total dC_m/dC_L of the X-1-2 airplane as obtained by summing up the contributions of the wing-fuselage combination and that of the horizontal tail is shown in figure 7. Since the major contribution is that of the horizontal tail, the variation with Mach number is very similar to that of the tail and, in turn, to $d\epsilon/d\alpha$. The few flight data available from preliminary transient response measurements made with the X-1-2 airplane have been plotted in the figure and are in reasonably good agreement with the values calculated. However, these data are limited to Mach numbers below that at which $\left(dC_m/dC_L\right)_A$ undergoes large changes and the data are insufficient to define the curve. From a comparison of the $\left(dC_m/dC_L\right)_A$ variation for the X-1-2 with that of the

X-1-1 shown in figure 3 it can be seen that the stability of both airplanes is about the same up to a Mach number of about 0.86. At Mach numbers above 0.86, however, the stability of the X-1-2 airplane is less than that of the X-1-1 by as much as 25 percent. The primary reason for this difference is found in the value of the ratio $C_{L_{\alpha_t}}/C_{L_{\alpha_w}}$ at Mach numbers greater than 0.86 for the two airplanes; for the X-1-1 the value is of the order of 1.1 while for the X-1-2 the value is about 0.90.

The apparent stability $d\delta_e/dC_{L_A}$ of the X-1-2 airplane was obtained from the expression

$$\frac{d\delta_e}{dC_{L_A}} = -\frac{\left(\dfrac{dC_m}{dC_L}\right)_A}{C_{L_{\alpha_t}} \dfrac{di_t}{d\delta_e} \dfrac{q_t}{q} \dfrac{S_t}{S} \dfrac{l_t}{c}}$$

The values for the various terms in this expression have been given in figures 4, 6, and 7. The variation of $d\delta_e/dC_{L_A}$ that would result from the changes experienced individually in $\left(dC_m/dC_L\right)_A$, $di_t/d\delta_e$, $C_{L_{\alpha_t}}$, and q_t/q are shown in figure 8 as obtained by holding all the other parameters constant at their value at $M = 0.75$ while the indicated quantity varied with Mach number. These curves indicate that the variation of elevator-stabilizer effectiveness is the most important change over the entire Mach number range except for a range between $M = 0.89$ and 0.96, where the change in static stability produces a greater change in $d\delta_e/dC_{L_A}$. The effects of the variations of $C_{L_{\alpha_t}}$ and q_t/q on $d\delta_e/dC_{L_A}$ are slight.

The variation of $d\delta_e/dC_{L_A}$ for the X-1-2 as computed by the equation presented in the previous paragraph is shown in figure 9. Points obtained in pull-ups in flight are shown in the same figure for comparison. These data show that reasonable agreement exists between the calculated variation and the flight data but that the calculated values are higher than the measured values. This difference may be caused by the uncertainty existing in the values of the C_{L_α} terms. The value of $d\delta_e/dC_{L_A}$ increases about twenty times as the Mach number is increased from 0.75 to 1.0. As may be seen from the preceding figure, this change is produced by the approximately five-fold decrease in $di_t/d\delta_e$, and the approximately three-fold increase in $\left(dC_m/dC_L\right)_A$. The variation of $d\delta_e/dC_{L_A}$ with Mach number has been extended above Mach number of 1.0 by means of the extrapolations shown in figure 8. It is indicated that at Mach numbers larger than 1.0 there is an appreciable decrease in $d\delta_e/dC_{L_A}$ shown in figures 6 and 7. This decrease in apparent stability is also shown by the few data available.

In actual level flight at constant altitude the pilot would not notice as large a change in the stability as shown in figure 9 because $d\delta_e/dg$ would increase by a factor of only 10 between $M = 0.7$ and $M = 1.0$ while $d\delta_e/dC_{L_A}$ increases by a factor of 20. This is because the lift coefficient required for level flight at a Mach number of 1.0 is half that required at $M = 0.7$.

Trim changes.- An attempt has been made to break down the trim changes reported for the X-1-2 airplane in reference 2. The trim equation in the form

$$C_{m_{c.g.}} = C_{m_o} + C_{L_A}\frac{x}{c} + C_{m_f} - \left\{i_t + \left(1 - \frac{d\epsilon}{d\alpha}\right)\left[\alpha_o + \frac{C_L}{\left(C_{L_\alpha}\right)_A}\right]\right\} C_{L_{\alpha t}} \frac{q_t}{q} \frac{S_t}{S} \frac{l_t}{c}$$

was used in the analysis.

The wing pitching moment about the aerodynamic center and the aerodynamic-center location were obtained from the pressure-distribution data presented in references 6 and 7. Curves of C_{m_o} and $C_{L_A}\,x/c$ for a lift coefficient of 0.3 are given in figure 10. A curve of α_o from reference 11 and unpublished flight data is shown in this figure as is the curve of $\alpha_o + \dfrac{C_L}{\left(C_{L_\alpha}\right)_A}$ for $C_L = 0.3$.

It was not possible to obtain the fuselage pitching-moment contribution for the X-1-2 because tail loads were not available for this airplane. However, the variation of tail incidence angle required for trim $\left(C_{m_{c.g.}} = 0\right)$ with zero elevator is available for the X-1-2 from reference 2. This curve is presented in figure 10 and will be used subsequently in the determination of the fuselage contribution.

The variation of the pitching moment produced by the horizontal tail at zero incidence was computed and is presented in figure 11. In order to show the effect of the downwash factor on this tail contribution, curves are shown for the pitching moment of the tail by using the variation of $d\epsilon/d\alpha$ shown in figure 5 and also by using a constant value of $\frac{d\epsilon}{d\alpha} = 0.59$. The data indicate that the negative value of the pitching moment first decreases slightly then increases with Mach number up to about 0.925 after which it decreases again. The curves indicate that the variation of $d\epsilon/d\alpha$ at Mach numbers above 0.86 is primarily responsible for the large negative value of the tail pitching moment at $M = 0.92$. If $d\epsilon/d\alpha$ were constant, the negative moment would decrease at Mach numbers larger than 0.87 rather than increasing and would have a value at $M = 1.0$ approximately half that indicated.

The variation of C_{m_F} obtained by solving the trim equation using the variation of tail incidence required for trim $\left(C_{m_{c.g.}} = 0\right)$ with zero elevator is shown in figure 11. This is actually not the variation of the fuselage-pitching moment alone but includes the variation of the pitching moment produced by the horizontal tail at zero incidence angle. The pitching moment is fairly constant to a Mach number of about 0.85 at which Mach number the nose-up value begins to increase rapidly to a value of 0.15 at $M = 1.0$.

The variation with Mach number of the total pitching-moment coefficient obtained by summing the contributions for the airplane with the tail incidence and elevator angle both at zero is presented in figure 11. The total pitching-moment coefficient decreases with Mach number from its value of 0.068 at $M = 0.78$ to a value near 0.042 at $M = 0.87$. At higher Mach numbers the pitching moment remains nearly constant.

The variation of trim elevator angle for any stabilizer setting may be computed by use of the trim equation which takes the form

$$\delta_e = \frac{C_{m_A}}{\frac{di_t}{d\delta_e} C_{L_{\alpha_t}} \frac{q_t}{q} \frac{S_t}{S} \frac{l_t}{c}} - \frac{i_t}{di_t/d\delta_e}$$

The effects of the variation with Mach number of $di_t/d\delta_e$, $C_{L_{\alpha_t}}$, and q_t/q were calculated for a tail incidence angle of 1.4° by holding two of the quantities constant at their value of $M = 0.75$ while the other quantity was varied. The results are presented in figure 12 and indicate that the change of $di_t/d\delta_e$ is primarily responsible for the change of trim with Mach number. The effects of $C_{L_{\alpha_t}}$ and q_t/q are slight. Also shown in figure 12 is a comparison of the calculated variation of elevator position for 1.4° stabilizer with the experimentally determined variation obtained from reference 2. The agreement is felt to be good except at $M = 0.99$ when the calculated value is about 1° less than the measured elevator required to trim.

CONCLUSIONS

As a result of the analysis presented herein the following conclusions have been reached for the X-1 airplanes at a lift coefficient of 0.3 at altitudes between 40,000 feet and 50,000 feet.

1. The value of the downwash factor $d\epsilon/d\alpha$ decreased from 0.59 at a Mach number of 0.80 to a minimum value of -0.19 at a Mach number of 0.925 followed by an increase to 0.20 at a Mach number of 1.0.

2. The tail dynamic-pressure ratio q_t/q varied but little with Mach number, decreasing to 0.925 at a Mach number of 0.84 followed by an increase to 0.96 at a Mach number of 0.93 and a decrease to 0.93 at a Mach number of 1.0.

3. The contribution of the fuselage to the static stability of the airplane $\left(dC_m/dC_L\right)_A$ was small and was not subject to large variations with Mach number.

4. The variation of the static-stability contribution of the horizontal tail dC_m/dC_L is similar to the variation in the downwash factor and is responsible for most of the variation in the static stability of the entire airplane.

5. The variation in apparent stability $d\delta_e/dC_{L_A}$ with Mach number was primarily caused by the large decrease in the relative elevator-stabilizer effectiveness $di_t/d\delta_e$ except between Mach number of 0.89 and 0.96 where the change in static stability produced by $d\epsilon/d\alpha$, the downwash factor, is the more important effect. The changes in these quantities result in an increase in apparent stability $d\delta_e/dC_{L_A}$ from a value of about 10° at a Mach number of 0.70 to a value of about 213° at a Mach number of 1.0 followed by a decrease to 130° at a Mach number of 1.05.

6. The positive value of the pitching moment for zero stabilizer and elevator decreases with increasing Mach number to a Mach number of 0.87 above which it is approximately constant.

7. The calculated trim curve is in good agreement with the experimentally determined variation of elevator angle with Mach number.

Langley Aeronautical Laboratory
National Advisory Committee for Aeronautics
Langley Field, Va.

REFERENCES

1. Drake, Hubert M., Goodman, Harold R., and Hoover, Herbert H.: Preliminary Results of NACA Transonic Flights of the XS-1 Airplane with 10-Percent-Thick Wing and 8-Percent-Thick Horizontal Tail. NACA RM L8I29, 1948.

2. Drake, Hubert M., and Carden, John R.: Elevator-Stabilizer Effectiveness and Trim of the X-1 Airplane to a Mach Number of 1.06. NACA RM L50G20, 1950.

3. Zalovcik, John A.: A Radar Method of Calibrating Airspeed Installations on Airplanes in Maneuvers at High Altitudes and at Transonic and Supersonic Speeds. NACA Rep. 985, 1950. (Formerly NACA TN 1979.)

4. Angle, Ellwyn E., and Holleman, Euclid C.: Determination of Longitudinal Stability of the Bell X-1 Airplane from Transient Responses at Mach Numbers up to 1.12 at Lift Coefficients of 0.3 and 0.6. NACA RM L50I06a, 1950.

5. Carman, L. Robert, and Carden, John R.: Lift and Drag Coefficients for the Bell X-1 Airplane (8-Percent-Thick Wing) in Power-Off Transonic Flight. NACA RM L51E08, 1951.

6. Carner, H. Arthur, and Payne, Mary M.: Tabulated Pressure Coefficients and Aerodynamic Characteristics Measured on the Wing of the Bell X-1 Airplane in Level Flight at Mach Numbers from 0.79 to 1.00 and in a Pull-Up at a Mach Number of 0.96. NACA RM L50H25, 1950.

7. Knapp, Ronald J., and Wilken, Gertrude V.: Tabulated Pressure Coefficients and Aerodynamic Characteristics Measured on the Wing of the Bell X-1 Airplane in Pull-Ups at Mach Numbers from 0.53 to 0.99. NACA RM L50H28, 1950.

8. Turner, Thomas R.: Maximum-Lift Investigation of a $\frac{1}{40}$-Scale X-1 Airplane Wing at Mach Numbers from 0.60 to 1.15. NACA RM L50C28, 1950.

9. Nelson, Warren H., and Erickson, Albert L.: The Effect of Aspect Ratio on the Subsonic Aerodynamic Characteristics of Wings with NACA 65_1-210 Sections. NACA RM A9K18, 1950.

10. Goodson, Kenneth W., and Morrison, William D., Jr.: Aerodynamic Characteristics of a Wing with Unswept Quarter-Chord Line, Aspect Ratio 4, Taper Ratio 0.6, and NACA 65A006 Airfoil Section. Transonic-Bump Method. NACA RM L9H22, 1949.

11. Mattson, Axel T., and Loving, Donald L.: Force, Static Longitudinal Stability, and Control Characteristics of a $\frac{1}{16}$-Scale Model of the Bell XS-1 Transonic Research Airplane at High Mach Numbers. NACA RM L8A12, 1948.

TABLE I

PHYSICAL CHARACTERISTICS OF BELL X-1 AIRPLANE

Engine:		Reaction Motors, Inc. model 6000C4
Rating, static thrust at sea level for each of the four rocket cylinders, lb		1,500
Propellant:		
Fuel		Diluted ethyl alcohol
Oxidizer		Liquid oxygen
Propellant flow (approx.), lb/sec/cylinder		7.9
Fuel feed		High pressure nitrogen gas
Weight:		
Maximum:		
With full load and incorporating 8-percent wing, lb		12,365
With full load and incorporating 10-percent wing, lb		12,200
Minimum:		
Landing condition, 8-percent wing, lb		7,340
Landing condition, 10-percent wing, lb		7,190
Moment of inertia (landing condition):	10-percent wing	8-percent wing
I_X, slug-ft^2	3,090	3,100
I_Y, slug-ft^2	11,710	12,350
I_Z, slug-ft^2	13,950	Not available
Center-of-gravity travel, percent mean aerodynamic chord		Maximum 22.1 percent full load to 25.3 percent empty
Over-all height, ft		10.85
Over-all length, ft		30.90
Wing:		
Area (including section through fuselage) sq ft		130
Span, ft		28
Airfoil section		NACA 65-110 (a = 1.0) and NACA 65-108 (a = 1.0)
Mean aerodynamic chord, in.		57.71
Location (aft of leading edge root chord), in.		6.58
Aspect ratio		6

NACA

TABLE I

PHYSICAL CHARACTERISTICS OF BELL X-1 AIRPLANE - Continued

Root chord, in.	74.2
Tip chord, in.	37.1
Taper ratio	2:1
Incidence, deg:	
Root	2.5
Tip	1.5
Sweepback (leading edge), deg	5.05
Dihedral (chord plane), deg	0
Wing flaps (plane):	
Area, sq ft	11.6
Span, ft	5.83
Chord (root), in.	14.84
Chord (tip), in.	10.58
Travel, deg	60
Aileron:	
Area (each aileron behind hinge line), sq ft	3.15
Span, ft	5.8
Travel, deg	±12
Chord, percent wing chord	15
Root-mean-square chord, ft	0.565
Horizontal tail:	
Section	NACA 65-008 and NACA 65-006
Area, sq ft	26.0
Span, ft	11.4
Aspect ratio	5
Distance from airplane design center of gravity to 25 percent mean aerodynamic chord of tail, ft	13.3
Stabilizer travel, deg (power actuated):	
Nose up	5
Nose down	10
Elevator (no aerodynamic balance):	
Area, sq ft	5.2
Travel from stabilizer, deg:	
Up	16
Down	7

Table I

PHYSICAL CHARACTERISTICS OF BELL X-1 AIRPLANE - Concluded

Root-mean-square chord, ft	0.464
Chord, percent horizontal-tail chord	20
Vertical tail:	
Area (excluding dorsal fin), sq ft	25.6
Total height above horizontal stabilizer, in.	61.25
Fin:	
Area (excluding dorsal fin), sq ft	20.4
Offset from thrust axis, deg	0
Rudder (no aerodynamic balance):	
Area, sq ft	5.2
Span, ft	6.58
Travel, deg	±15
Root-mean-square chord, ft	0.798
Chord, percent vertical-tail chord	20

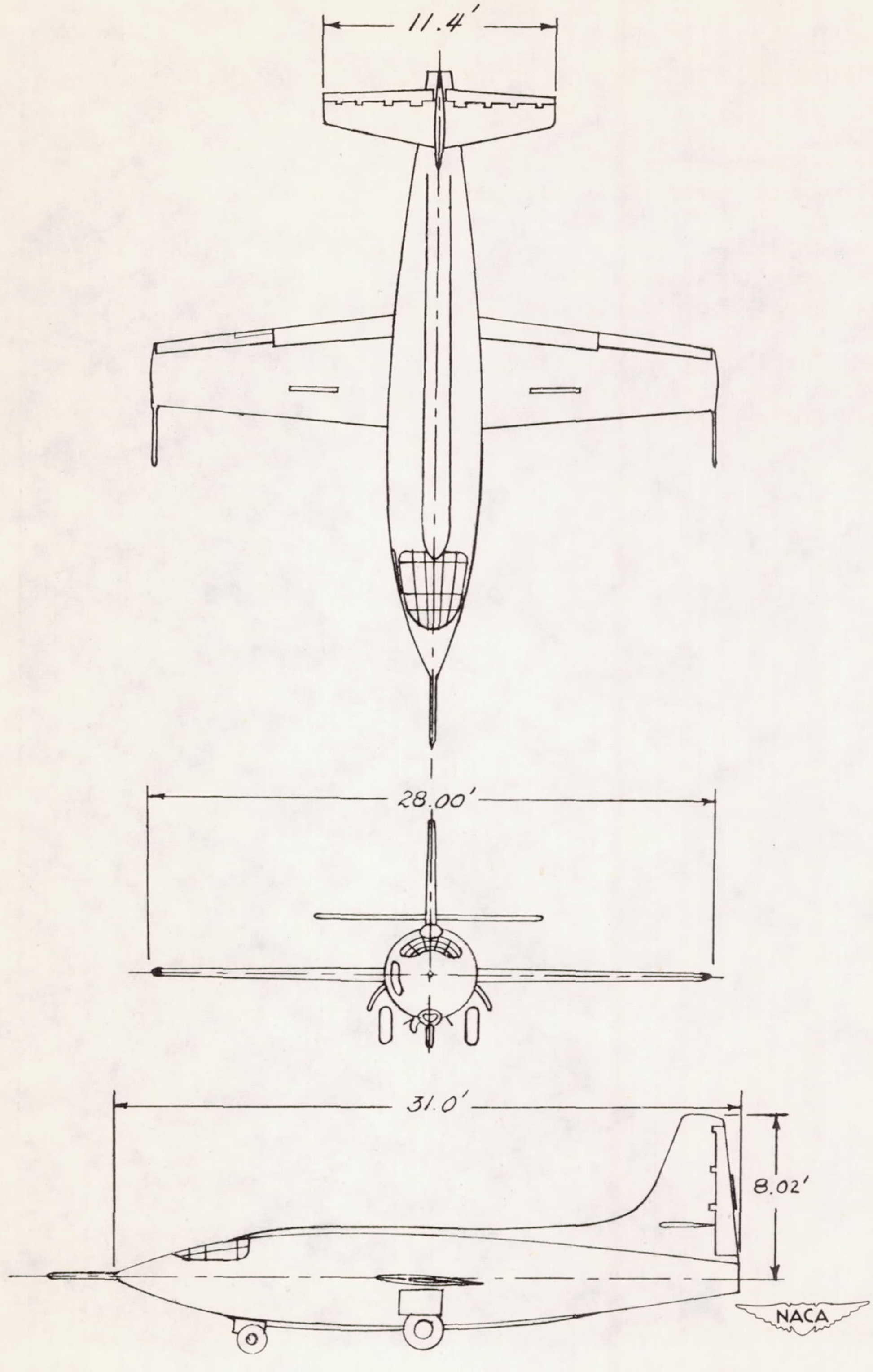

Figure 1.- Three-view drawing of X-1 airplane.

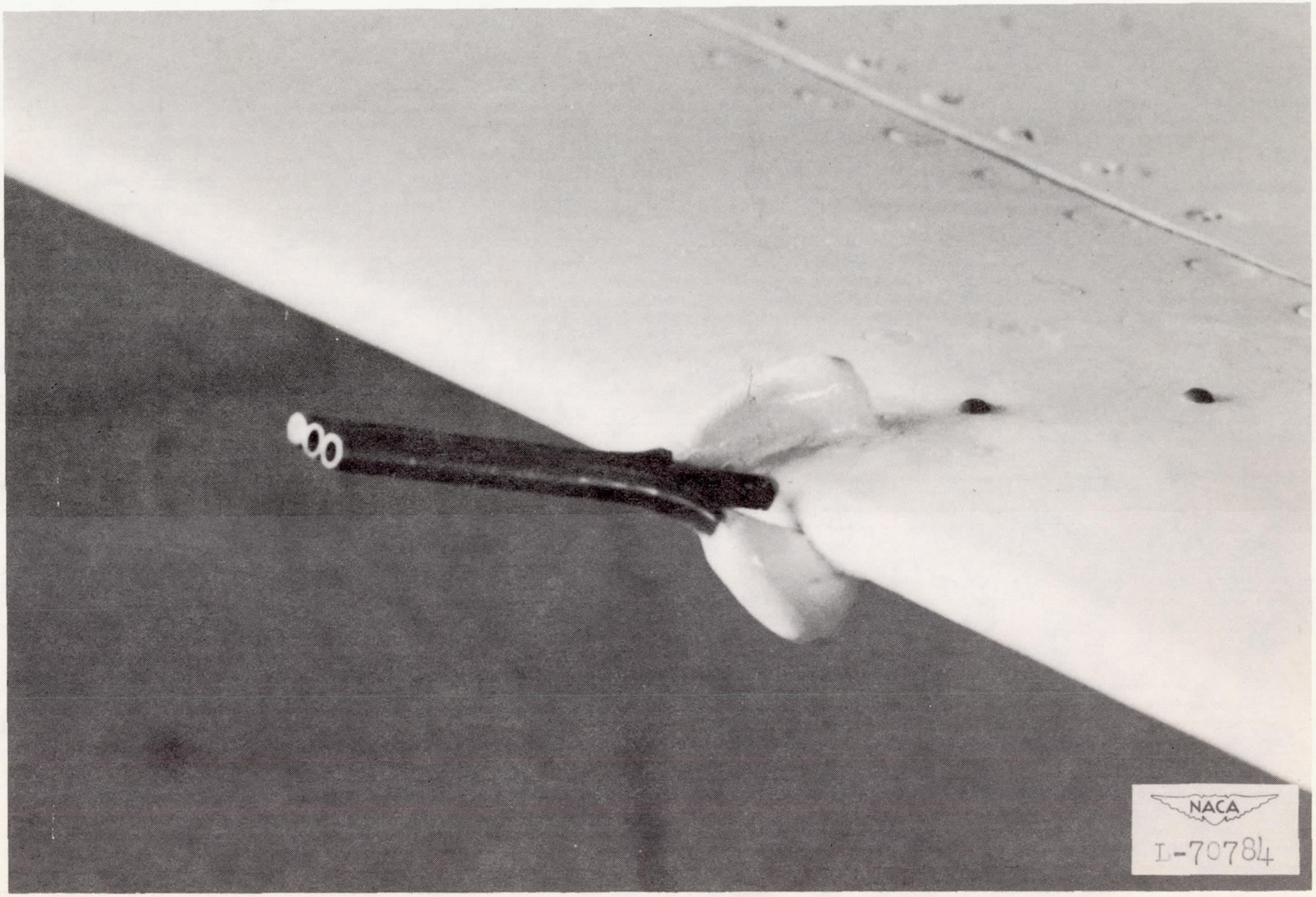

Figure 2.- Photograph of tail total-pressure installation on the X-1-2 airplane.

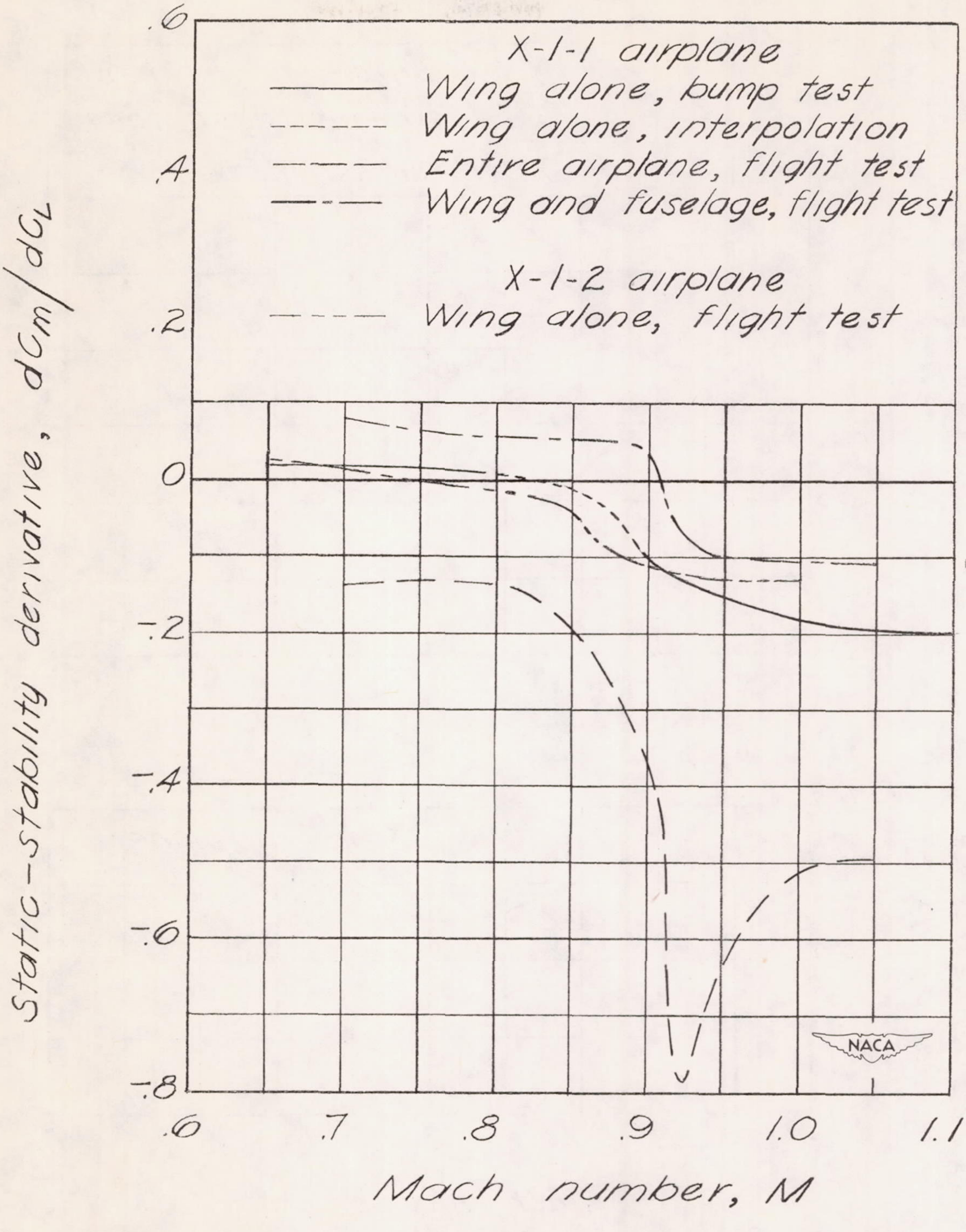

Figure 3.- Variation of the static-stability derivative with Mach number for portions of the X-1 airplanes. $C_L = 0.3$; center of gravity at 23.5 percent mean aerodynamic chord.

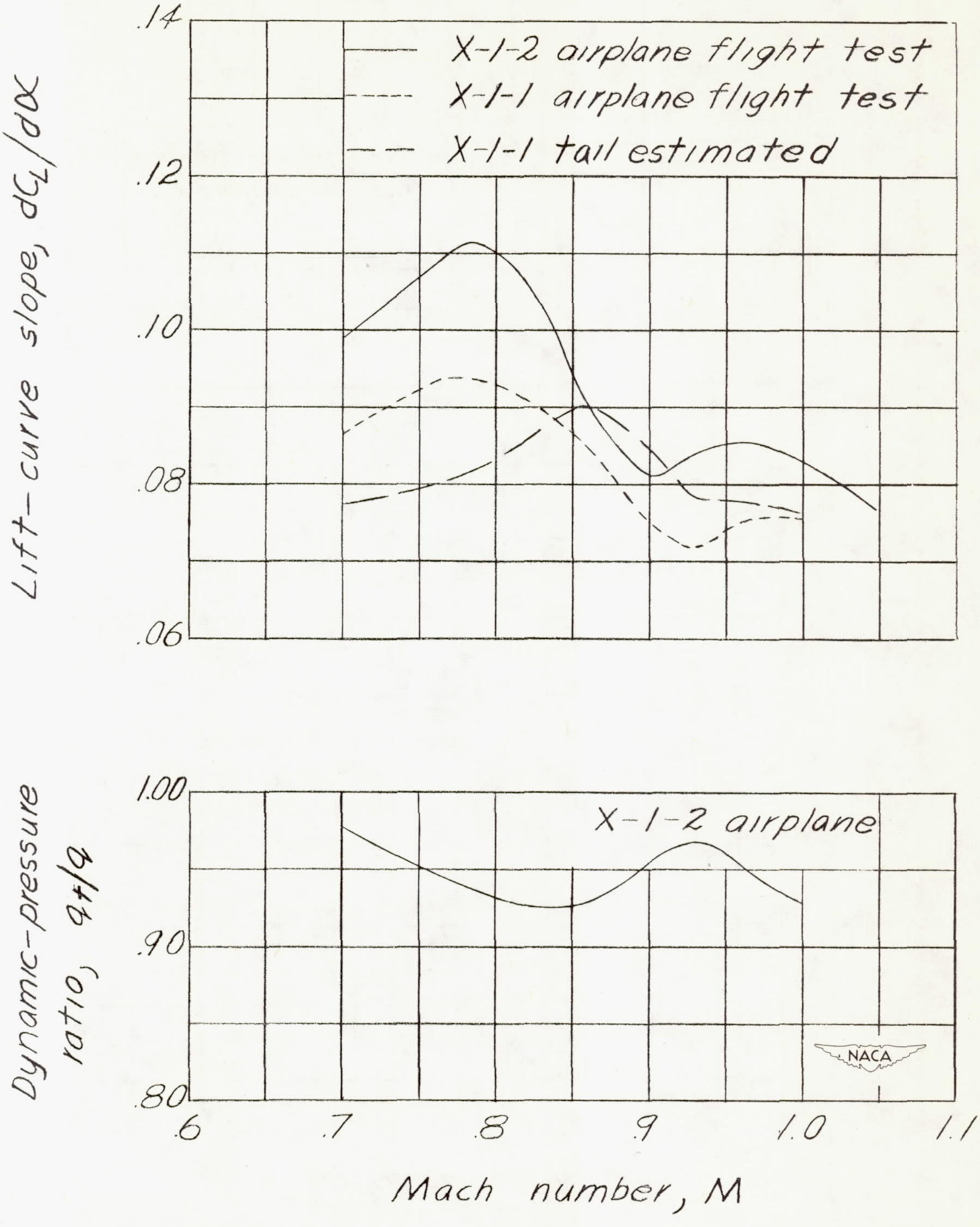

Figure 4.- Variation of lift-curve slopes and tail dynamic-pressure ratio with Mach number for X-1 airplanes.

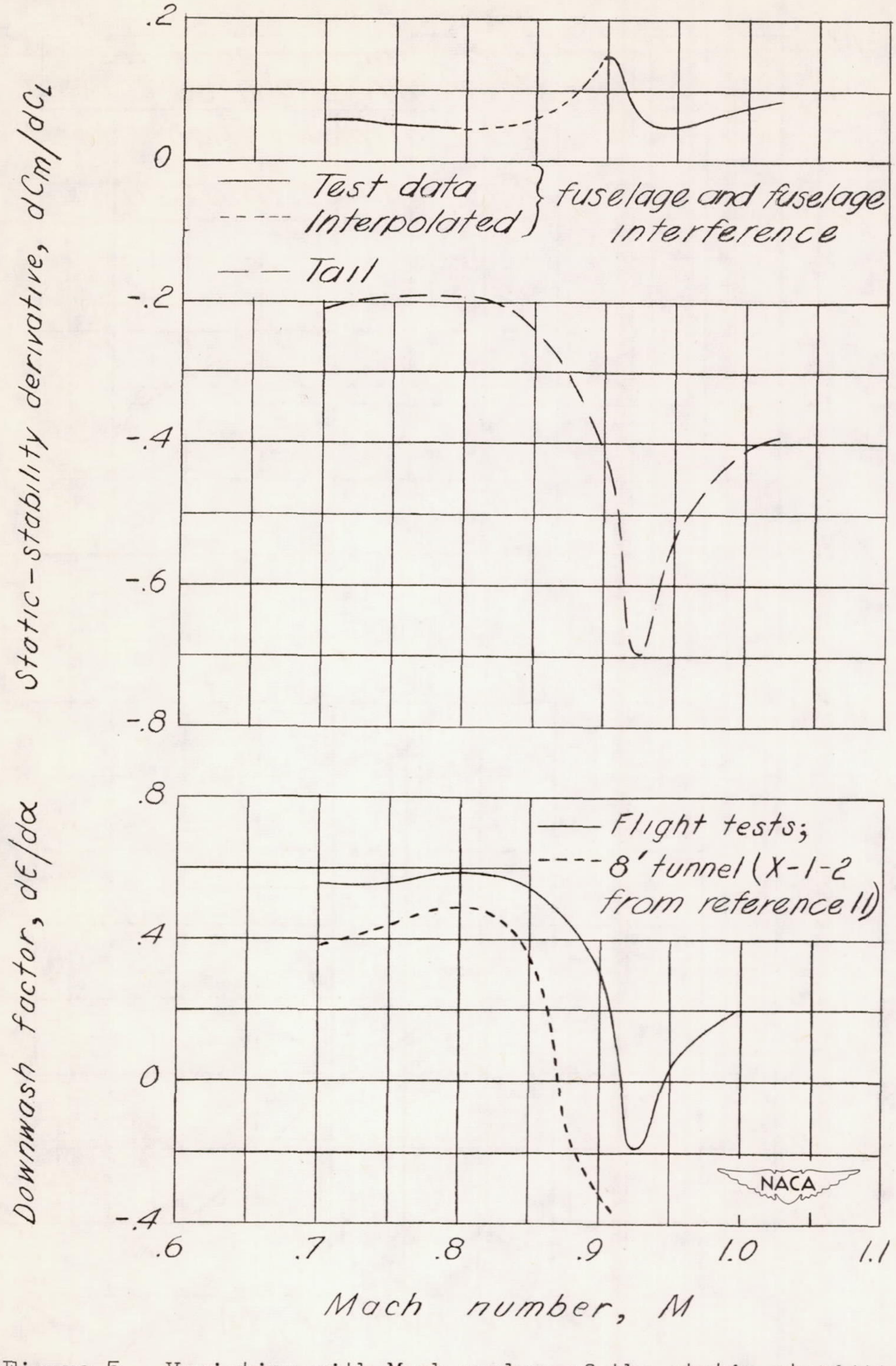

Figure 5.- Variation with Mach number of the static-stability contributions of fuselage and tail and computed downwash factor for X-1-1 airplane. $C_L = 0.3$; center of gravity at 23.5 percent mean aerodynamic chord.

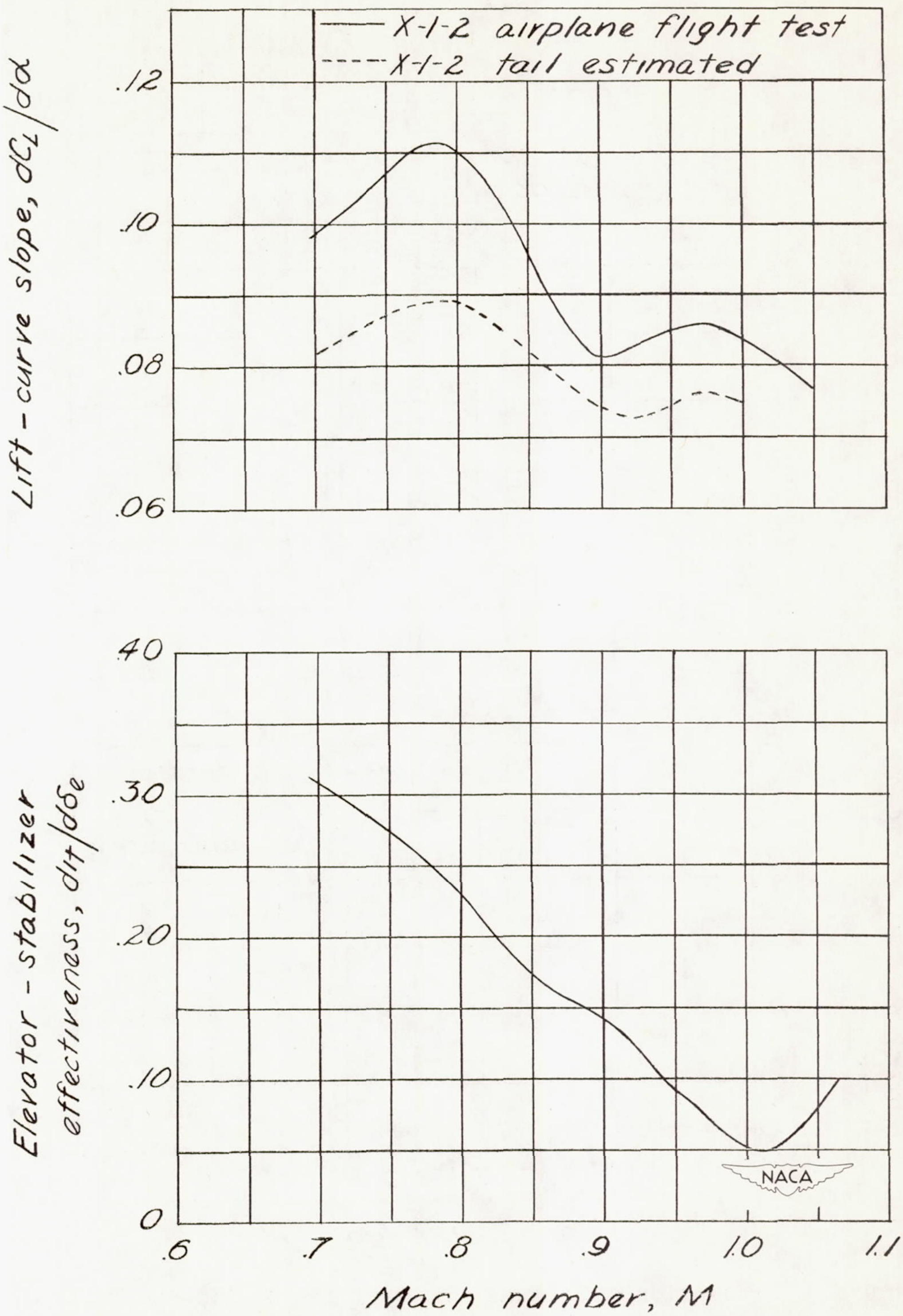

Figure 6.- Variation of lift-curve slopes and relative elevator-stabilizer effectiveness with Mach number for X-1-2 airplane. $C_L = 0.3$.

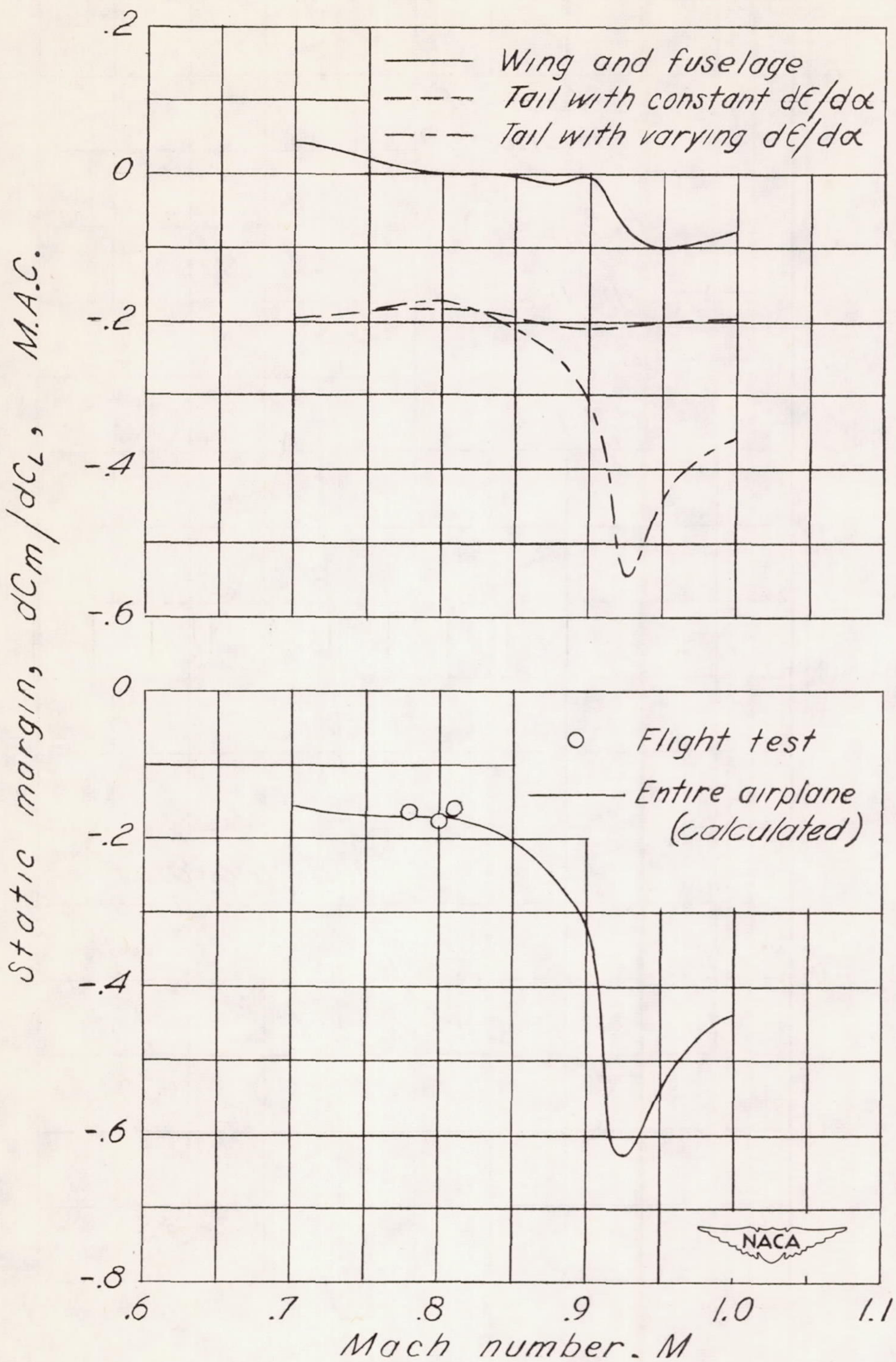

Figure 7.- Static-stability contributions of various parts of X-1-2 airplane and total airplane static-stability variation with Mach number. $C_L = 0.3$; center of gravity at 22 percent mean aerodynamic chord.

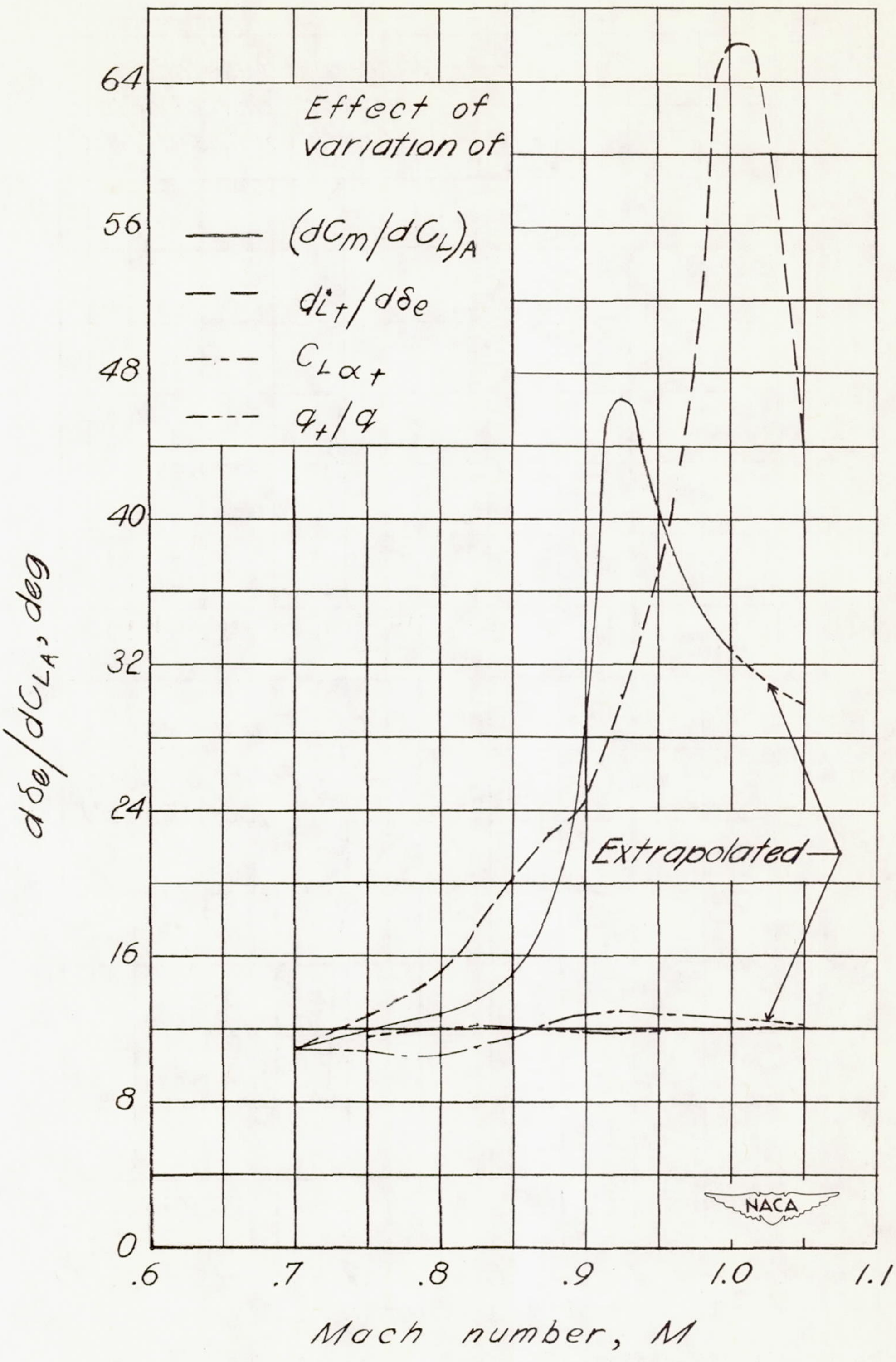

Figure 8.- Effects on elevator effectiveness of X-1-2 of variations of several quantities with Mach number. $C_L = 0.3$; center of gravity at 22 percent mean aerodynamic chord.

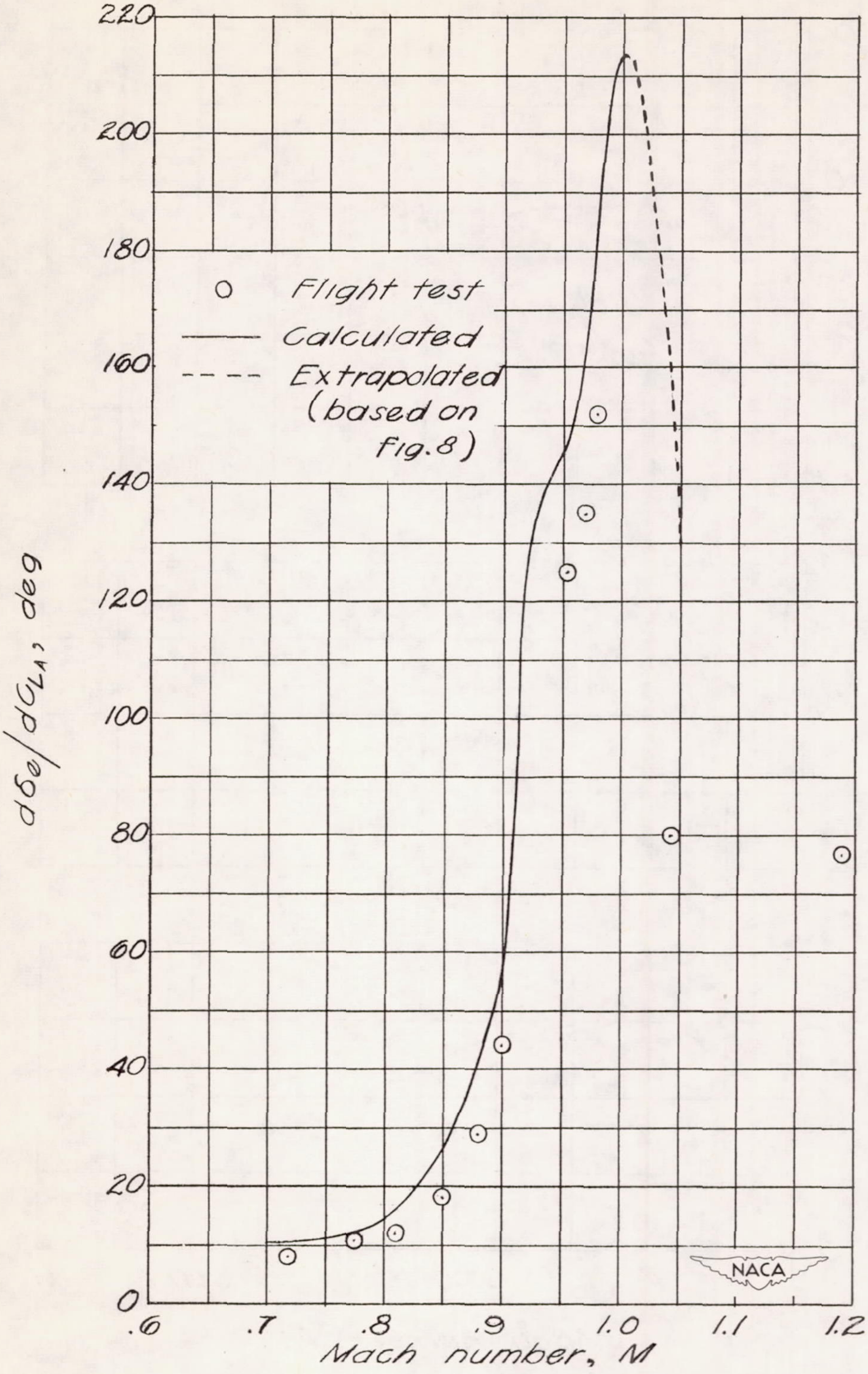

Figure 9.- Variation of elevator effectiveness in producing lift with Mach number for X-1-2. Center of gravity at 22 percent mean aerodynamic chord.

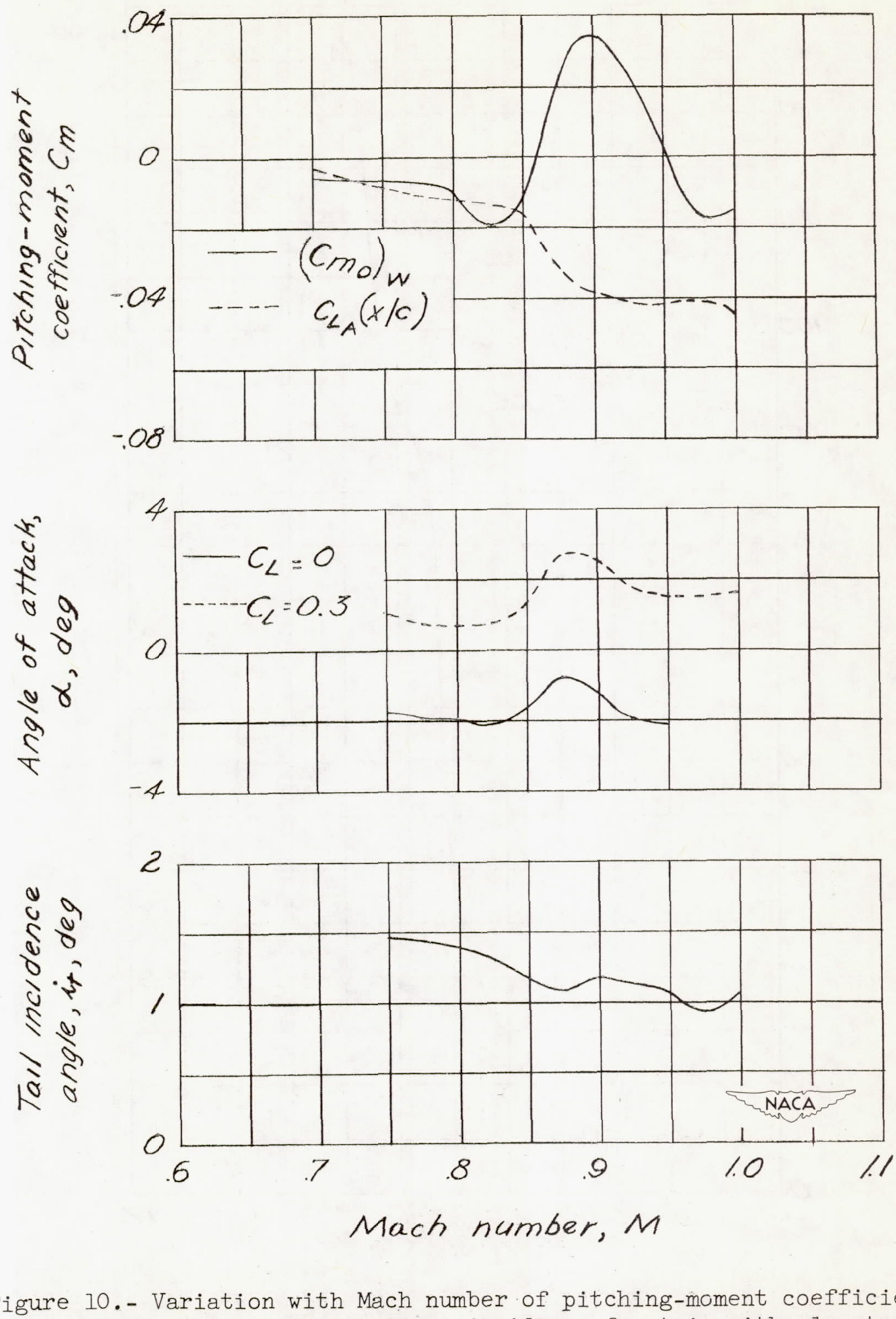

Figure 10.- Variation with Mach number of pitching-moment coefficient, angle of attack, and stabilizer incidence for trim with elevator zero for X-1-2 airplane. Center of gravity at 22 percent mean aerodynamic chord; altitude, 40,000 feet.

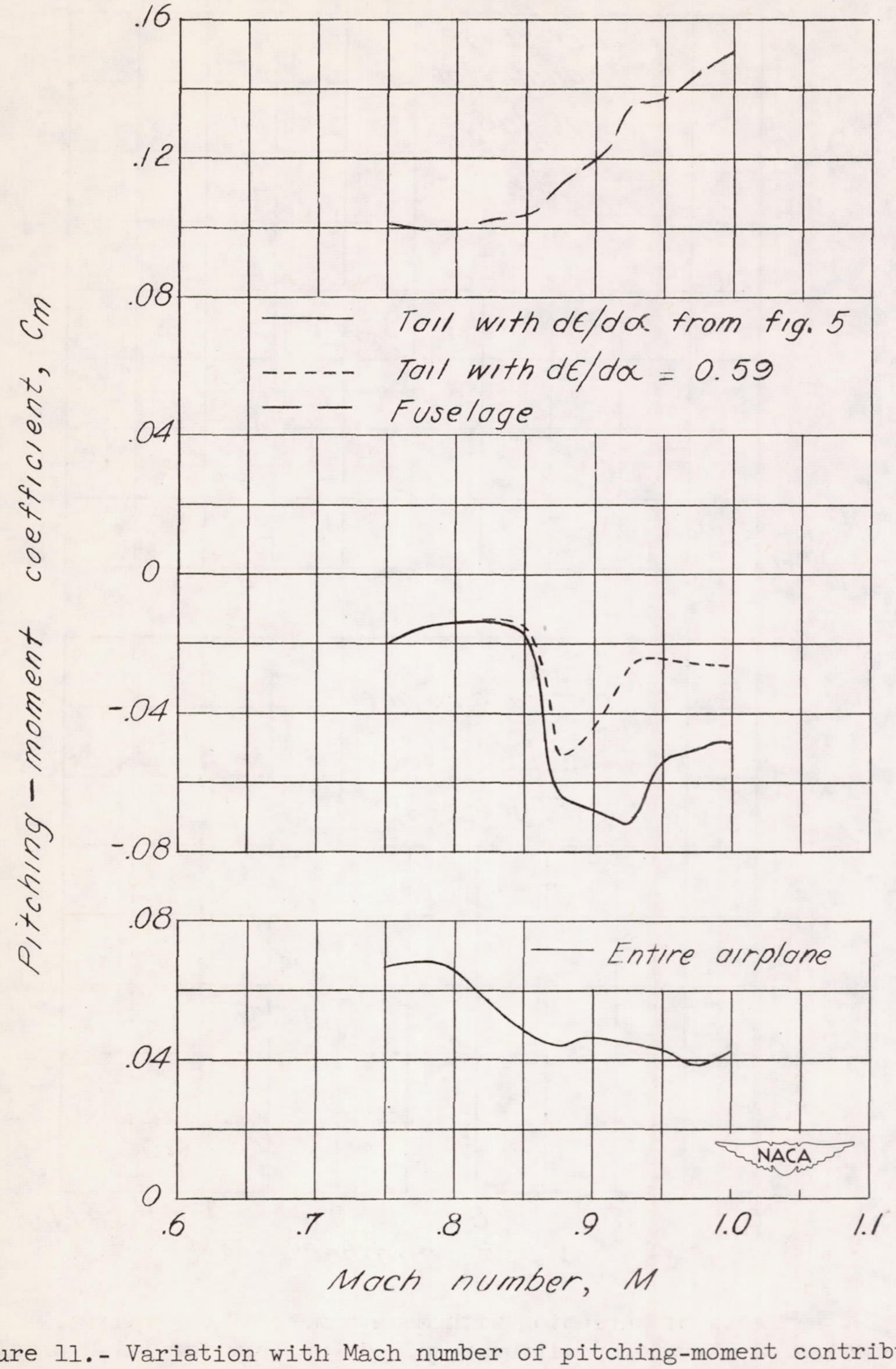

Figure 11.- Variation with Mach number of pitching-moment contributions of tail and fuselage with $i_t = \delta_e = 0$ and total airplane pitching moment for X-1-2. $C_L = 0.3$; center of gravity at 22 percent mean aerodynamic chord; altitude, 40,000 feet.

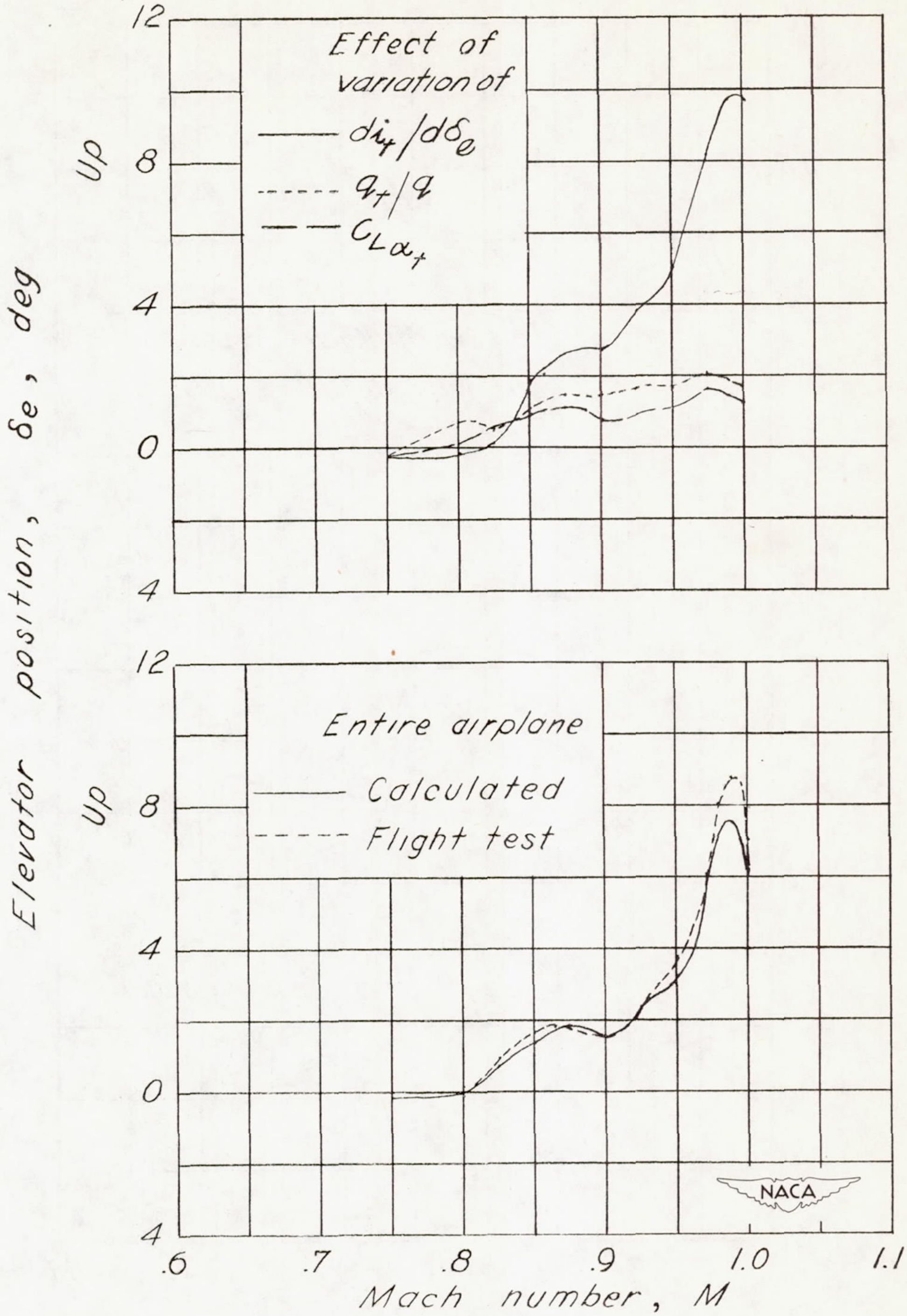

Figure 12.- Effects of variation with Mach number of several tail parameters on elevator position required for trim for X-1-2 airplane and variation with Mach number of trim elevator angle for the entire airplane. $i_t = 1.4^{\circ}$; $C_L = 0.3$; center of gravity at 22 percent mean aerodynamic chord; altitude, 40,000 feet.